Radiative heavy quark energy loss in an expanding viscous QCD plasma

Sreemoyee Sarkar,[1] Chandrodoy Chattopadhyay,[2] and Subrata Pal[2]
[1]*Centre for Excellence in Basic Sciences, University of Mumbai, Vidyanagari Campus, Mumbai 400098, India*
[2]*Department of Nuclear and Atomic Physics, Tata Institute of Fundamental Research, Homi Bhabha Road, Mumbai 400005, India*

(Received 3 January 2018; published 21 June 2018)

We study viscous effects on heavy quark radiative energy loss in a dynamically screened medium with boost-invariant longitudinal expansion. We calculate, to first order in opacity, the energy loss by incorporating viscous corrections in the single-particle phase-space distribution function within relativistic dissipative hydrodynamics. We consider Grad's 14-moment and the Chapman-Enskog-like methods for the nonequilibrium distribution functions. Our numerical results for the charm quark radiative energy loss show that, as compared to an expanding ideal (nonviscous) fluid, viscosity in the evolution leads to somewhat enhanced energy loss which is rather insensitive to the underlying viscous hydrodynamic models used. Further inclusion of a viscous correction induces larger energy loss, and the magnitude and pattern of this enhancement crucially depend on the form of viscous corrections used.

DOI: 10.1103/PhysRevC.97.064916

I. INTRODUCTION

High-energy heavy-ion collision experiments at the Relativistic Heavy-Ion Collider (RHIC) [1,2] and the Large Hadron Collider (LHC) [3–5] have firmly established the formation of strongly interacting matter composed of a color deconfined system of quarks and gluons. Such a conclusion was partly based on relativistic viscous hydrodynamic analysis of the large anisotropic flow that requires a remarkably small shear viscosity to entropy density ratio of $\eta/s = 0.08$–0.20 [6–9]. This not only suggests that the matter formed is close to local thermal equilibrium, but also provides a window to the initial state of the fireball immediately after the collision. Hydrodynamic and transport models have been widely used to study the properties of the hot and dense medium by exploring the collective flow of the soft (bulk) hadrons.

On the other hand, the suppression of high transverse momentum of light and heavy quarks produced in hard processes provides an excellent tool that allows tomographic studies of the QCD plasma [10–15]. The suppression is caused by the attenuation (energy loss) of the energetic partons via inelastic and elastic collisions during their propagation in the medium. Heavy quarks, in particular, provide a promising probe as these are formed in the early stages via hard scatterings, and their production in the plasma at later stages is largely suppressed owing to their large mass [15]. These primordial heavy quarks could thus explore various stages of the space-time evolution.

The energy loss of energetic partons was originally expected to be dominated by medium-induced gluon radiation [16,17]. More recent and consistent collisional energy loss calculations suggest that the radiative and collisional energy losses of heavy quarks are comparable at low and moderate transverse momenta p_T [18] and at $p_T \gtrsim 15$ GeV/c the collisional energy loss (although becomes progressively smaller than radiative) can have important contributions to jet quenching [19]. Moreover, at low p_T, the phase space for the medium-induced gluon radiation becomes restricted due to large quark mass (the "dead cone effect") in contrast to light partons [20]. Consequently, RHIC measurements of the heavy flavor suppression data for $p_T \lesssim 8$ GeV/c [21] can be reasonably well reproduced by various models that include distinct parton energy loss formalisms as well as radial flow and charm quark hadronization via recombination; see Ref. [22] and references therein. On the other hand, heavy-ion collisions at the LHC enable D-meson measurements from low to a much higher p_T up to 100 GeV/c [22,23] and thus provide the ideal ground to study heavy flavor suppression.

A surprisingly large suppression pattern of high-p_T D mesons, similar to that for charged hadrons, was observed at the LHC and quantified by the nuclear modification factor of $R_{AA} = (dN/dp_T)_{AA}/N_{\rm bin}(dN/dp_T)_{pp}$, defined as the ratio of the yield in AA and pp collisions scaled by the number of binary nucleon-nucleon collisions. The solution of this heavy flavor puzzle is traced to the interplay between the bare partons' suppression and the fragmentation function with identical suppression of the bare charm (equal to D-meson suppression) and light quarks (unexpectedly coinciding with charged hadrons suppression) as predicted by perturbative QCD [24]. However, the crucial ingredient for a reliable suppression prediction relies on a precise energy loss calculation taking due consideration of the expansion and viscosity of the QCD medium.

Early calculations of the medium-induced radiative energy loss were based on a "static QCD medium" consisting of randomly distributed static scattering centers. In such a static medium, the collisional energy loss exactly vanishes. Subsequently, the radiative energy loss in a dynamically screened QCD medium was developed for an optically thin infinite [25] and finite-size [26,27] plasma, more relevant for rapidly expanding a medium formed in relativistic heavy-ion collisions. Radiative energy loss in a plasma was also shown to receive corrections because of modified dielectric effect of the medium known as the Ter-Mikayelian effect [28]. Furthermore, the calculation of radiative energy loss suffers a complication due to the Landau-Pomeranchuck-Migdal (LPM) effect [29–31] which introduces a controlled reduction of emitted gluon formation time.

The existing calculations on energy loss have been performed purely for an ideal fluid using the equilibrium phase-space distribution function and ignoring viscous effects. Since the quark-gluon plasma (QGP) formed in relativistic heavy-ion collisions behaves like a near-perfect fluid with a small η/s, it is imperative to account for the viscous effects in computing the radiative energy loss. In fact, the importance of viscosity of the medium has already been realized in several quantities or observables relevant for the RHIC and the LHC, such as the heavy quark damping rate [32], anisotropic flow [6–9], event-plane correlations [33,34], dilepton spectra [35,36], etc. Although few calculations have incorporated radiative energy loss only for viscous medium evolution [13,37], a realistic and consistent calculation where viscosity is explicitly included in the computation of energy loss as well as in the expanding viscous medium is crucial.

In this paper, we present the first calculation of radiative energy loss with viscosity, in first order in opacity, of a heavy (charm) quark in a dynamically screened viscous QCD medium that undergoes boost-invariant longitudinal expansion. The energy-loss computation has been performed for an infinite-size QCD viscous medium and the complications of finite-size (LPM) effects are ignored. We employ causal second-order viscous hydrodynamics for the underlying evolution of the medium based on the Müller-Israel-Stewart (MIS) framework [38–40] and the recently derived dissipative equations from the Chapman-Enskog- (CE-) like approach of iteratively solving the Boltzmann equation in the relaxation-time approximation [41–43]. Viscous effects are incorporated in the single-particle distribution $f(x,p) = f_0(x,p) + \delta f_{\rm vis}(x,p)$ via the nonequilibrium distribution function $\delta f_{\rm vis}$. The single-particle distribution would modify the scattering cross section of the energetic parton with the medium and thereby the radiative energy loss. For the nonequilibrium distribution, we use the commonly used form based on Grad's 14-moment approximation [44] and that obtained from the Chapman-Enskog method. We will show that viscosity, in general, enhances the energy loss and the enhancement is significant in Grad's method. Furthermore, we find nonlinearity in the time dependence of the radiative energy loss for a viscous plasma, which mimics the energy-loss behavior due to coherent gluon radiation.

The paper is organized as follows. In Sec. II we introduce the dissipative hydrodynamic formalisms used and then compute in these models, to first order in opacity, the radiative energy loss in a dynamical viscous QCD medium with boost-invariant longitudinal expansion. In Sec. III we compare the results for the radiative energy loss in ideal and viscous fluids and with further inclusion of viscous corrections due to the Grad and Chapman-Enskog methods by using initial conditions relevant to that produced in heavy-ion collisions at the LHC. A summary and conclusions are presented in Sec. IV. The technical details of the calculation of gluon self-energies is given in Appendix A, and the computations of energy loss are presented in Appendices B–D.

II. RADIATIVE ENERGY LOSS IN AN EXPANDING VISCOUS MEDIUM

In this section we compute the medium-induced heavy flavor radiative energy loss in the boost-invariant longitudinal expansion of matter within second-order viscous hydrodynamics. The hydrodynamic evolution is governed by the conservation of energy-momentum tensor $\partial_\mu T^{\mu\nu} = 0$, where

$$T^{\mu\nu} = \epsilon u^\mu u^\nu - P\Delta^{\mu\nu} + \pi^{\mu\nu}. \tag{1}$$

We will work in the Landau-Lifshitz frame and disregard particle flow $N^\mu = n_B u^\mu + V^\mu$ due to very small values of net-baryon number n_B and net-charge flow V^μ at the RHIC and the LHC [40,45]. In the above equation, ϵ and P, respectively, are the energy density and pressure in the fluid's local rest frame (LRF), and $\pi^{\mu\nu}$ is the shear pressure tensor. $\Delta^{\mu\nu} = g^{\mu\nu} - u^\mu u^\nu$ is the projection operator on the three-space orthogonal to the hydrodynamic four-velocity u^μ defined by the Landau-matching condition $T^{\mu\nu}u_\nu = \epsilon u^\mu$.

For Bjorken longitudinal expansion, we work with the Milne coordinates (τ,x,y,η_s) where the proper time is $\tau = \sqrt{t^2 - z^2}$, the space-time rapidity is $\eta_s = \ln[(t+z)/(t-z)]/2$, and the four-velocity is $u^\mu = (1,0,0,0)$. The conservation equation for the energy-momentum tensor gives the evolution of ϵ,

$$\frac{d\epsilon}{d\tau} = -\frac{1}{\tau}(\epsilon + P - \Phi), \tag{2}$$

where $\Phi \equiv -\tau^2\pi^{\eta_s\eta_s}$ is taken as the independent component of the shear pressure tensor. For the three independent variables, we need two more equations, namely, the viscous evolution equation and the equation of state (EoS). In this paper, we have used a conformal QGP fluid EoS with thermodynamic pressure $P = \epsilon/3$. The simplest choice for the dissipative equation would be the relativistic Navier-Stokes theory where the instantaneous constituent equation for the shear pressure in the Bjorken case gives

$$\Phi = \frac{4\eta}{3}\theta. \tag{3}$$

Here $\eta \geqslant 0$ is the shear viscosity coefficient, and the local expansion rate is $\theta = 1/\tau$. However, this first-order theory suffers from acausality and instability.

The most commonly used second-order dissipative hydrodynamic equation, derived from positivity of the divergence of the entropy four-current, is based on the works of MIS [38–40]. In the boost-invariant scaling expansion, the MIS dissipative equation,

$$\frac{d\Phi}{d\tau} + \frac{\Phi}{\tau_\pi} = \frac{4\eta}{3\tau_\pi}\theta - \lambda_\pi\theta\Phi \tag{4}$$

restores causality by enforcing the shear pressure to relax to its first-order value via the relaxation-time $\tau_\pi = 2\eta\beta_2$, where β_2 is the second-order transport coefficient. In the present paper we consider $\tau_\pi = 2\eta\beta_2 = 5\eta/(sT)$ corresponding to that obtained in a weakly coupled QCD [46–49]. Furthermore, the coefficient of the second-order term (in the expansion of the velocity gradients) for the EoS of an ultrarelativistic gas is $\lambda_\pi = 4/3$.

In the derivation of Eq. (4) pertaining to a system that is out of equilibrium, the nonequilibrium effects have been quantified via the phase-space distribution $f(x,p) = f_0(x,p) + \delta f_{\rm vis}(x,p)$ where the nonequilibrium part of the distribution function $\delta f_{\rm vis}(x,p)$ is usually obtained by expanding $f(x,p)$ about the equilibrium distribution function $f_0(x,p) \approx [\exp(u\cdot p/T) - 1]^{-1}$. Grad's 14-moment approximation [44] is the common choice for the viscous correction in hydrodynamics where the expansion in powers of momenta is truncated at quadratic order. For a system of massless particles in the absence of bulk viscosity and charge diffusion current, Grad's method for the viscous correction gives

$$\delta f_{\rm vis} = f_0(1\pm f_0)\frac{\pi_{\mu\nu}p^\mu p^\nu}{2(\epsilon+P)T^2}, \\ \equiv f_0(1\pm f_0)\frac{3\Phi}{4(\epsilon+P)T^2}\left(\frac{\vec{\mathbf{p}}^2}{3} - p_z^2\right), \quad (5)$$

where the second line is the equivalent representation for boost-invariant longitudinal expansion (assumed to be along the z direction) of the fluid in the LRF [50]. This equation has been exclusively used in deriving the second-order MIS dissipative equation.

Alternatively, dissipative evolution equations can be obtained from the CE method by perturbative expansion of the Boltzmann transport equation using the Knudsen number as a small expansion parameter [41–43]. By expanding the nonequilibrium distribution function $\delta f_{\rm vis}$ about the local equilibrium value and iteratively solving the Boltzmann equation in the relaxation-time approximation, the second-order dissipative equation for the shear tensor in the boost-invariant case has the same form as that of Eq. (4) for the MIS case. However, in the Chapman-Enskog-like approach, the relaxation time naturally comes out to be $\tau_\pi = 2\eta\beta_2 = 5\eta/(sT)$ and $\lambda_\pi = 38/21$ [41]. The corresponding nonequilibrium distribution function has the form

$$\delta f_{\rm vis} = f_0(1\pm f_0)\frac{5\pi_{\mu\nu}p^\mu p^\nu}{8PT(u\cdot p)}, \\ \equiv f_0(1\pm f_0)\frac{15\Phi}{16PT(u\cdot p)}\left(\frac{\vec{\mathbf{p}}^2}{3} - p_z^2\right). \quad (6)$$

We will present the calculational details of heavy quark radiative energy loss for the Müller-Israel-Stewart dissipative hydrodynamics with Grad's form of $\delta f_{\rm vis}(x,p)$. The results within the Chapman-Enskog approach can be obtained in a similar fashion, which will be presented at the end of this section.

We will compute the energy loss in a dynamical QCD medium for a thin expanding plasma in the opacity expansion. In a nonexpanding plasma the energy loss is calculated by expansion over the number of parton scatterers in the medium times the transport cross section, integrated over the path-length L traversed by the heavy quark. In an expanding medium, the total energy loss is obtained by summing the instantaneous energy loss over the time spent by the quark in the plasma before reaching vacuum or the survival time in the plasma.

In principle, boost-invariant expansion induces anisotropy in the medium, hence the energy lost by a quark depends on its direction of propagation relative to the fluid flow [51]. In this paper, we consider the propagation of the heavy quark to be along the fluid direction and relegate to future work the calculation of complicated directional dependence of energy loss. As in Ref. [25], we restrict ourselves to first order in opacity where an on-shell heavy quark of mass M and spatial momentum $\vec{\mathbf{p}} \gg M$ produced in the remote past traverses along fluid flow, i.e., the z direction. On scattering with a parton in the medium, it exchanges a virtual gluon of momentum $q = (q_0,\vec{\mathbf{q}}) = (q_0,q_z,\mathbf{q})$ and radiates a gluon with momentum $k = (\omega,\vec{\mathbf{k}}) = (\omega,k_z,\mathbf{k})$. The heavy quark then emerges along the z direction with a momentum $p' = (E',\vec{\mathbf{p}}') = (E',p_z',\mathbf{p}')$. As the gluon momentum is spacelike ($q_0 \leqslant |\vec{\mathbf{q}}|$) and the radiated gluon momentum is timelike ($\omega \geqslant |\vec{\mathbf{k}}|$), these contribute accordingly in the gluon propagators $D^{\mu\nu}(q)$ and $D^{\mu\nu}(k)$, respectively. The validity of a soft gluon ($\omega \ll E$) and soft rescattering ($|\mathbf{q}| \sim |\mathbf{k}| \ll k_z$), approximations at high-temperature T at the LHC together with the energy-momentum conservation $p = p' + k + q$ enable us to write

$$k = \left(\omega \approx k_z + \frac{\mathbf{k}^2 + m_g^2}{2k_z}, k_z, \mathbf{k}\right), \\ p' = \left(E' \approx p_z' + \frac{\mathbf{p}'^2 + M^2}{2p_z'}, p_z', -(\mathbf{k}+\mathbf{q})\right), \quad (7) \\ p = \left(E \approx p_z' + k_z + q_z + \frac{M^2}{2(p_z' + k_z + q_z)}, p_z' + k_z + q_z, \mathbf{0}\right).$$

Here $m_g \approx \mu/\sqrt{2} \sim gT/\sqrt{2}$ is the effective gluon mass in a thermalized QGP at temperature T with Debye screening mass μ.

The heavy quark energy loss per unit proper time τ, to first order in opacity, can be obtained by folding the heavy quark interaction rate $\Gamma(E)$ with the energy-loss $\omega + q_0$ and averaging over the initial color of the quarks [52,53],

$$\frac{dE_{\rm dyn}}{d\tau} = \frac{1}{D_R}\int d\omega\,\omega\frac{d\Gamma(E)}{d\omega} \approx \frac{E}{D_R}\int dx\,x\frac{d\Gamma(E)}{dx}. \quad (8)$$

The soft rescattering approximation $\omega + q_0 \approx \omega$ has been used, and x is the longitudinal momentum fraction of the quark carried by the emitted gluon. D_R is defined as $[t_a,t_c][t_c,t_a] = C_2(G)C_R D_R$ with $C_2(G) = 3$, $D_R = 3$, and $[t_a,t_c]$ is a color commutator. The interaction rate is given by

$$\Gamma(E) = \frac{1}{2E}2\,{\rm Im}\,\mathcal{M}_{\rm tot}, \\ = \frac{1}{2E}(2\,{\rm Im}\,\mathcal{M}_{1,0} + 2\,{\rm Im}\,\mathcal{M}_{1,1} + 2\,{\rm Im}\,\mathcal{M}_{1,2}), \quad (9)$$

which can be obtained by computing all the Feynman diagrams (see Appendices B–D) that contribute at first order in opacity for the radiative energy loss. $\mathcal{M}_{1,0}$, $\mathcal{M}_{1,1}$, and $\mathcal{M}_{1,2}$ are the corresponding loop diagrams of the scattering amplitudes where, zero, one, and two ends of the radiated gluon k are attached to the exchanged gluon q (see Figs. 7–9 for illustration).

In the high-temperature plasma, the exchanged gluon receives a correction from medium partons. This many-body effect gets encoded in the hard thermal loop (HTL) gluon propagators [54]. The effective 1-HTL gluon propagator has the form [55,56]

$$iD_{\mu\nu}(l) = \frac{P_{\mu\nu}(l)}{l^2 - \Pi_T(l)} + \frac{Q_{\mu\nu}(l)}{l^2 - \Pi_L(l)}, \tag{10}$$

where the gluon-momentum $l = (l_0,\vec{\mathbf{l}})$ and the transverse $P^{\mu\nu}(l)$ and longitudinal $Q^{\mu\nu}(l)$ projectors in the Coulomb gauge have the nonzero components $P^{ij}(l) = -\delta^{ij} + l^i l^j/\vec{\mathbf{l}}^2$ and $Q^{00}(l) = -l^2/\vec{\mathbf{l}}^2$. In an expanding viscous QCD plasma, the longitudinal Π_L and transverse Π_T gluon self-energies in Grad's approximation are given by [see Eq. (A5) in Appendix A],

$$\Pi_L(l) = \Pi_L^0(l) - \frac{3\Phi}{4sT^3}\frac{2g^2}{(2\pi)^2}\int \mathbf{p}^3 d\mathbf{p}\, dy\, \mathcal{G}(\mathbf{p}) \times \frac{1-3y^2}{3(1-y)^2}\frac{|\vec{\mathbf{l}}|y}{l_0 - |\vec{\mathbf{l}}|y}, \tag{11}$$

$$\Pi_T(l) = \Pi_T^0(l) - \frac{3\Phi}{4sT^3}\frac{g^2}{(2\pi)^2}\int \mathbf{p}^3 d\mathbf{p}\, dy\, \mathcal{G}(\mathbf{p}) \times \frac{1-3y^2}{3(1-y)^2}\frac{|\vec{\mathbf{l}}|(1-y)}{l_0 - |\vec{\mathbf{l}}|y}. \tag{12}$$

The ideal part of polarizations $\Pi^0_{L,T}$ is given in Eq. (A6). The phase-space factor $\mathcal{G}(\mathbf{p}) = N_f\{\exp[g(\mathbf{p})]+1\}^{-1} + N_c\{\exp[g(\mathbf{p})]-1\}^{-1}$ with $g(\mathbf{p}) \equiv \mathbf{p}/(T\sqrt{1-y^2})$ can be expressed in terms of the dimensionless variable of Eq. (A3), viz. $y = |\vec{\mathbf{p}}|\cos\theta_p(\tau_0/\tau)[\vec{\mathbf{p}}^2\cos^2\theta_p(\tau_0/\tau)^2 + \vec{\mathbf{p}}^2]^{-1/2}$. For typical values of $\eta/s \lesssim 3/(4\pi)$ (required to explain flow data at the RHIC and the LHC), inclusion of viscous corrections in $\Pi_{L,T}$ is found to increase the radiative energy loss by at most $\sim 3\%$.

The imaginary part of the exchanged gluon propagator is

$$D^>_{\mu\nu}(q) = [1+f(q)]2\,\mathrm{Im}\left[\frac{P_{\mu\nu}(q)}{q^2 - \Pi_T(q)} + \frac{Q_{\mu\nu}(q)}{q^2-\Pi_L(q)}\right] \times \theta\left(1 - \frac{q_0^2}{\vec{\mathbf{q}}^2}\right). \tag{13}$$

The distribution function $f(q) = f_0(q) + \delta f_{\rm vis}(q)$ receives a strong viscous correction of $\delta f_{\rm vis}(q)$ due to Grad's 14-moment approximation of Eq. (5); the equilibrium gluon momentum distribution function is $f_0(q) = [\exp(q_0/T) - 1]^{-1}$. For the radiated gluon, $\Pi_L(k) \approx 0$ and $\Pi_T(k) \approx m_g$. Using the soft scattering limit ($\omega \gg |\mathbf{q}| \sim |\mathbf{k}| \sim gT$), and noting that $f(k) \ll 1$ for energetic partons [25], the cut propagator for the imaginary part of the radiated gluon becomes

$$D^>_{\mu\nu}(k) \approx -2\pi\frac{P_{\mu\nu}(k)}{2\omega}\delta(k_0 - \omega), \tag{14}$$

where $\omega \approx \sqrt{\vec{\mathbf{k}}^2 + m_g^2}$. The cut propagator for the heavy quark is

$$D^>(p') \approx 2\pi\frac{1}{2E'}\delta(p'_0 - E'). \tag{15}$$

With the help of these propagators one can calculate the matrix amplitude squared for the diagrams (see Appendices B–D). The phase-space factor for the cut diagrams receives in-medium viscous corrections. On computing the diagrams and in conjunction with Eqs. (8) and (9), one can obtain the heavy quark radiative energy loss. The contribution to the energy loss from the first set of diagrams $2\,\mathrm{Im}\,\mathcal{M}_{0,1}$ [see Eq. (B9)] is given by

$$\left.\frac{1}{E}\frac{dE}{d\tau}\right|_{1,0} = \frac{3\alpha_s^2 C_R T}{\pi^3}\int dx\, d^2\mathbf{k}\, d^2\mathbf{q}\frac{\mathbf{k}^2}{(\mathbf{k}^2+\chi)^2}\Lambda(\tau,\mathbf{q}), \tag{16}$$

where $\chi = M^2x^2 + m_g^2$ and the strong-coupling constant $\alpha_s = g^2/(4\pi)$. The medium information is encoded within the quantity,

$$\Lambda(\tau,\mathbf{q}) = \int dy\left(1 + \frac{\Phi}{4sT^3}\frac{\mathbf{q}^2(1-3y^2)}{1-y^2}\right)\mathcal{F}_{LT}(\mathbf{q},y), \equiv \Lambda_0(\tau,\mathbf{q}) + \delta\Lambda_{\rm vis}(\tau,\mathbf{q}), \tag{17}$$

where $\Lambda_0(\tau,\mathbf{q})$ and $\delta\Lambda_{\rm vis}(\tau,\mathbf{q})$ stem from an ideal and viscous correction due to Grad's 14-moment approximation (5) for the $P = \epsilon/3$ equation of state. We have used the short-hand notation $\mathcal{F}_{LT} \equiv \mathcal{F}_L - \mathcal{F}_T$ for the difference in the polarization tensors $\mathcal{F}_Z = 2\,\mathrm{Im}\,\Pi_Z(y)\{[\mathbf{q}^2 + \mathrm{Re}\,\Pi_Z(y)]^2 + [\mathrm{Im}\,\Pi_Z(y)]^2\}^{-1}$ with $Z \equiv (L,T)$. It is evident from the energy-loss expression, that the nature of divergence gets modified from the ideal to the viscous Bjorken case due to an extra $\mathbf{q}^2$ factor stemming from $\delta\Lambda_{\rm vis}$.

The diagram $\mathcal{M}_{1,2}$ where emission of a gluon occurs from the exchanged gluon has been computed in Appendix C. The corresponding radiative energy loss is given by [see Eq. (C4)]

$$\left.\frac{1}{E}\frac{dE}{d\tau}\right|_{1,2} = \frac{3\alpha_s^2 C_R T}{\pi^3}\int dx\, d^2\mathbf{k}\, d^2\mathbf{q}\frac{(\mathbf{k}+\mathbf{q})^2}{[(\mathbf{k}+\mathbf{q})^2+\chi]^2}\Lambda(\tau,\mathbf{q}). \tag{18}$$

Finally, the diagrams for $\mathcal{M}_{1,1}$ can be computed as the product of the previous two diagrams $\mathcal{M}_{1,0}$ and $\mathcal{M}_{1,2}$. The resulting radiative energy loss gives [Eq. (D6) in Appendix D]

$$\left.\frac{1}{E}\frac{dE}{d\tau}\right|_{1,1} = \frac{3\alpha_s^2 C_R T}{\pi^3}\int dx\, d^2\mathbf{k}\, d^2\mathbf{q} \times \frac{-2\mathbf{k}\cdot(\mathbf{k}+\mathbf{q})}{[(\mathbf{k}+\mathbf{q})^2+\chi][\mathbf{k}^2+\chi]}\Lambda(\tau,\mathbf{q}). \tag{19}$$

The total energy loss is obtained by summing Eqs. (16), (18), and (19) as

$$\begin{aligned}\frac{1}{E}\frac{dE}{d\tau} &= \frac{\alpha_s C_R}{\pi^3\lambda_{\rm dyn}}\int dx\, d^2\mathbf{k}\, d^2\mathbf{q} \times\left[\frac{\mathbf{k}}{\mathbf{k}^2+\chi} - \frac{\mathbf{k}+\mathbf{q}}{[(\mathbf{k}+\mathbf{q})^2+\chi]}\right]^2\Lambda(\tau,\mathbf{q}),\\ &\equiv \frac{\alpha_s C_R}{\pi^3\lambda_{\rm dyn}}\int dx\, d^2\mathbf{k}\, d^2\mathbf{q}\,\mathcal{P}_g(x,\mathbf{k},\mathbf{q})\Lambda(\tau,\mathbf{q}).\end{aligned} \tag{20}$$

In the above equation, a dynamical mean free path has been defined as $\lambda_{\rm dyn}^{-1} = C_2(G)\alpha_s T = 3\alpha_s T$. In contrast to a time-independent QCD medium [25–27] where $\lambda_{\rm dyn}$ is constant, in the present expanding medium $\lambda_{\rm dyn}$ and thereby the density of scatterers has a time dependence via the temperature which modifies the energy loss.

Using the Chapman-Enskog results for the viscous evolution equation and the corresponding nonequilibrium distribution function (6), the total radiative energy loss can

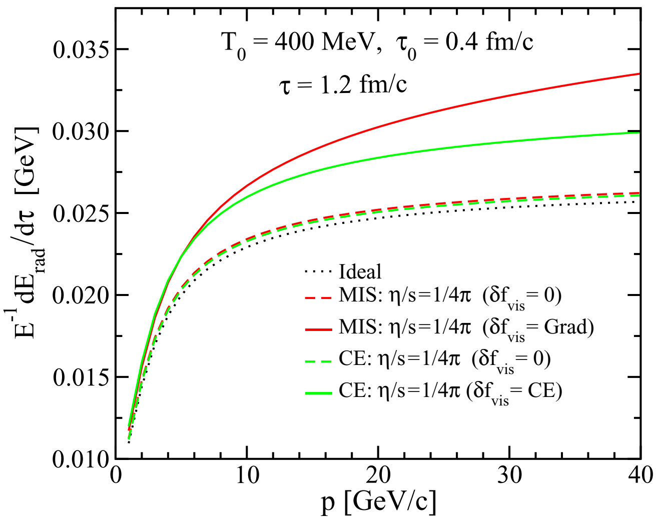

FIG. 1. Fractional differential radiative energy loss as a function of momentum for charm quarks in a boost-invariant expanding plasma at time $\tau = 1.2$ fm/c. The results are for an ideal fluid (black dotted line) in the dissipative hydrodynamics without a viscous correction in the MIS (red dashed line) and CE (green dashed line) theories and with further inclusion of the viscous correction due to Grad in the MIS (red solid line) and Chapman-Enskog (green solid line) methods. The results are for an ideal gas equation of state ($P = \epsilon/3$) with an initial temperature of $T_0 = 400$ MeV, a proper time of $\tau_0 = 0.4$ fm/c, and a constant shear viscosity to entropy density ratio of $\eta/s = 1/4\pi$.

be shown to have the same form as Eq. (20) in Grad's approximation. However, in the CE method, the quantity Λ of (17) is replaced by

$$\Lambda(\tau,\mathbf{q}) = \int dy\left(1 + \frac{5\Phi}{4sT^2}\frac{\mathbf{q}(1-3y^2)}{1-y^2}\right)\mathcal{F}_{LT}(\mathbf{q},y), \quad (21)$$

which involves the nonequilibrium form of the distribution function in the CE method.

III. RESULTS AND DISCUSSIONS

In this section we estimate numerical effects of expanding viscous medium on the radiative energy loss in first order in opacity for a dynamically screened QCD medium. We consider a plasma with an initial temperature of $T_0 = 400$ MeV and a proper time of $\tau_0 = 0.4$ fm/c that corresponds to (averaged) values obtained in Pb + Pb collisions at the LHC center-of-mass energy $\sqrt{s_{NN}} = 2.76$ TeV. The charm quark of mass $M = 1.2$ GeV is assumed to traverse in the plasma that has an effective number of degrees of freedom $N_f = 3$ with a fixed strong-coupling constant $\alpha_s = g^2/4\pi = 0.3$.

In boost-invariant longitudinal expansion of an ideal fluid, the temperature decreases with time as $T = T_0(\tau_0/\tau)^{1/3}$. The momentum dependence of the fractional differential energy-loss $E^{-1}dE/d\tau$ of the charm quark is shown at time $\tau = 1.2$ fm in Fig. 1 (black dotted line) in this ideal hydrodynamics. With the inclusion of dissipation in the dynamical evolution, the temperature decreases at a slower rate, and the entropy increases as compared to an inviscid fluid. In Fig. 1 we present the fractional differential radiative energy loss of a charm quark in an expanding viscous medium with $\eta/s = 1/4\pi$ at $\tau = 1.2$ fm/c in the MIS (red dashed lined) and the CE (green dashed line) methods in the absence of the nonequilibrium part of the distribution function obtained by setting $\delta f_{\rm vis} \sim \delta\Lambda_{\rm vis} = 0$ in Eq. (20). Dissipative effects are seen to cause an $\sim$5% larger energy loss for charm quarks with momentum $p \geqslant 10$ GeV as compared to that with ideal flows. Such an enhanced energy loss may be attributed to a relatively higher instantaneous temperature of the viscous plasma. Although the temperature in the CE method falls slightly faster with time as compared to that in the MIS theory, the energy losses in these viscous evolution frameworks are found to be practically insensitive.

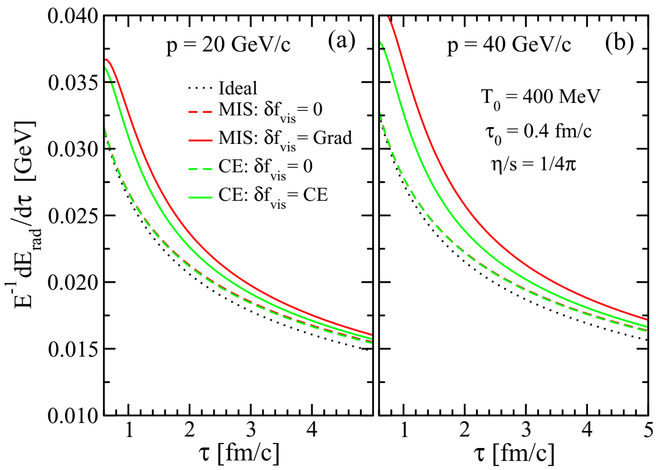

FIG. 2. Time dependence of fractional differential radiative energy loss for charm quarks of initial momentum $p = 20$ and 40 GeV/c. The initial conditions and the various curves are the same as in Fig. 1.

Figure 1 also shows the fractional differential energy loss obtained by inclusion of viscous corrections in the single-particle distribution function using the Grad (red solid line) and Chapman-Enskog (green solid line) methods at $\tau = 1.2$ fm/c. We find that a nonequilibrium correction induces a significant increase in the energy loss, the enhancement being particularly large for Grad's 14-moment approximation as compared to the Chapman-Enskog correction for heavy quark momentum $p \gtrsim 10$ GeV/c. This can be understood by comparing the (positive) contribution from viscous correction $\delta f_{\rm vis}$ to the energy loss in the Grad and Chapman-Enskog approaches, namely, Eqs. (17) and (21). An extra factor of $\mathbf{q}/5T$ in the integrand of $\delta\Lambda_{\rm vis}(\tau,\mathbf{q})$ in Grad's method gives a larger energy loss and results in a slower rate of saturation of fractional differential energy loss with the momentum p of the charm quark. On the other hand, the energy loss obtained in the Chapman-Enskog viscous correction shows a similar saturation pattern as that seen in an ideal fluid and in a viscous medium with $\delta f_{\rm vis} = 0$. At $p < 10$ GeV/c the energy loss has an identical behavior for the two viscous corrections used here. Large viscous corrections due to Grad's 14-moment approximation have been also found in the spectra and elliptic flow of hadrons at kinetic freezeout [6,45,57] as well as in the longitudinal Hanbury-Brown-Twiss radii of pions [42].

Figure 2(a) displays the proper time dependence of fractional differential radiative energy loss $E^{-1}dE/d\tau$ for a charm

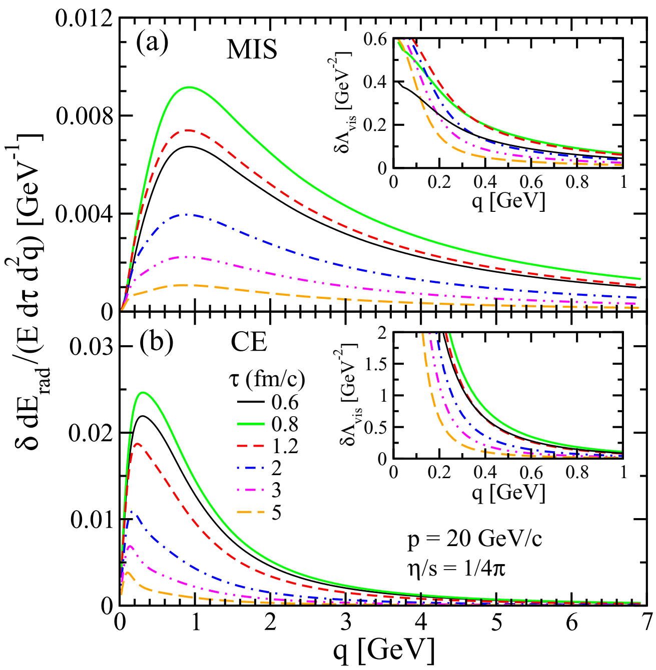

FIG. 3. Dissipative part of the differential fractional energy loss $\delta dE/(E\,d\tau\,d\mathbf{q})$ as a function of exchanged gluon momentum $\mathbf{q}$ at various proper times for charm quarks of initial momentum $p = 20$ GeV$/c$ at $\eta/s = 1/4\pi$ in the MIS and CE methods. The inset shows the variation of viscous correction $\delta\Lambda_{\rm vis}(\tau,\mathbf{q})$ with momentum $\mathbf{q}$ at various times. The initial conditions are the same as in Fig. 1.

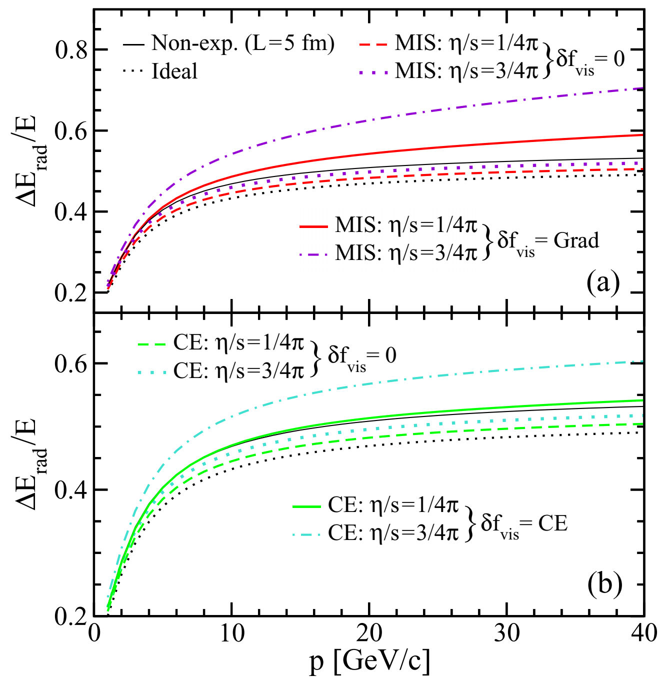

FIG. 4. Time-integrated fractional radiative energy loss as a function of momentum for charm quarks propagating in a boost-invariant expanding fluid over a total time of $\tau_f = 5$ fm$/c$ with various values of η/s in the MIS (top panel) and CE (bottom panel) frameworks. In a nonexpanding plasma at a temperature of $T_0 = 0.228$ GeV, the fractional energy loss integrated over a path length of $L = 5$ fm is also shown (black thin solid line). The initial conditions and the various curves for the expanding medium are the same as in Fig. 1. In addition, results with $\eta/s = 3/4\pi$ are shown without viscous corrections in MIS (purple dotted line) and CE (cyan dotted line) theories and with further inclusion of viscous corrections in MIS (purple dashed-dotted line) and CE (cyan dashed-dotted line) methods.

quark of momentum $p = 20$ GeV$/c$. With increasing time, the decrease in the energy loss is essentially due to falling temperatures. As compared to viscous hydrodynamics, in ideal hydrodynamic evolution the temperature decreases faster with time resulting in smaller energy loss at all times. At early times $\tau \lesssim 3$ fm$/c$, larger viscous drag in MIS hydrodynamics results in higher temperatures as compared to CE and hence gives the largest energy loss. At later times (lower temperature) all the viscous fluids give nearly identical energy losses mainly due to negligibly small shear pressure tensor Φ in the dilute medium. Of course, for charm quarks with momentum $p > 20$ GeV$/c$, the differences in $E^{-1}dE/d\tau$ will sustain at long times as evident from Fig. 2(b) for $p = 40$ GeV$/c$.

To gauge the kinematic contribution from the viscous correction $\delta\Lambda_{\rm vis}(\tau,\mathbf{q})$ on the radiative energy loss in the MIS and CE approaches, we show in Fig. 3 the viscous part of the fractional differential energy loss $\delta\,dE/(E\,d\tau\,d^2\mathbf{q})$ as a function of exchange gluon momentum $\mathbf{q}$ at various proper times. In both of these approaches, the effects of the dissipative correction first increase and then decrease with time (following the variation in shear stress) until the fluid attains local thermodynamic equilibrium. At a given time, the fractional differential energy loss with an increase in the gluon momentum $\mathbf{q}$ exhibits a gradual rise followed by a slow fall in the MIS theory. In contrast, the CE approach leads to a faster buildup of $\delta\,dE/(E\,d\tau\,d^2\mathbf{q})$ and rapid decrease with increasing $\mathbf{q}$. The differences in the energy-loss pattern and magnitude are essentially due to the extra factor of $\mathbf{q}/5T$ in the viscous correction in the MIS method as compared to the CE method [see Eqs. (17) and (21)]. In fact, these features can be traced to the variation in the viscous correction $\delta\Lambda_{\rm vis}(\tau,\mathbf{q})$ (see the inset of Fig. 3), which decreases smoothly with increasing $\mathbf{q}$ in the MIS, as compared to the sharper fall from very large values in the CE method. Consequently, the ($\mathbf{q}$-integrated) fractional energy-loss $dE/(E\,d\tau)$ receives a larger contribution in the MIS theory as seen in Figs. 1 and 2.

We show, in Fig. 4, the charm quark momentum dependence of the fractional radiative energy loss $\Delta E/E$ at various values of η/s in the MIS and CE theories with initial values of $\tau_0 = 0.4$ fm$/c$ and $T_0 = 0.400$ GeV. The total ΔE is obtained by summing the energy loss during the entire time traversed by the quark. In the present calculation we set this time as $\tau_f = 5$ fm$/c$ as the typical lifetime of the QGP phase at the RHIC and the LHC. On the other hand, in a nonexpanding fluid, the ΔE shown here refers to energy loss integrated over a path length of $L = 5$ fm. This result was obtained at a temperature of $T_0 = 0.228$ GeV corresponding to the average value obtained in the ideal hydrodynamic evolution from the initial $\tau_0 = 0.4$ fm$/c$ to the final $\tau_f = 5$ fm$/c$ and approximates a nonexpanding medium calculation [25]. At this (lower) averaged temperature, the integrated energy loss for the nonexpanding medium is found to be somewhat larger than that found in ideal hydrodynamics initialized at a higher temperature. As compared to a nonexpanding fluid, in an expanding medium the scattering rates decrease with time resulting in smaller $\Delta E/E$. However, large viscous corrections give a positive contribution to the energy loss that grows with η/s, especially when the nonequilibrium part of the distribution function in Grad's approximation is considered.

It may be mentioned that the fractional energy loss so obtained [by τ integration of Eq. (20)] has explicit temperature dependence via the dynamical mean free path $\lambda_{\rm dyn}^{-1}(T)$ and viscous correction $\delta\Lambda_{\rm vis}(\tau,\mathbf{q})$. The above computed energy loss with and without $\delta\Lambda_{\rm vis}(\tau,\mathbf{q})$ compares solely to the temperature-dependent contribution from the viscous correction. The effects of temperature-dependent $\lambda_{\rm dyn}^{-1}$ have been assessed by computing $\Delta E/E$ with a fixed $\lambda_{\rm dyn}$ corresponding to a time-averaged temperature of $T \approx 0.235$ GeV in the MIS and CE approaches (figure not shown). Here the other quantities, including $\delta\Lambda_{\rm vis}(\tau,\mathbf{q})$ [corresponding to Eq. (20)], follow the underlying temperature evolution of the system. This result should be then compared with that for T-varying $\lambda_{\rm dyn}(T)$ and $\delta\Lambda_{\rm vis}(\tau,\mathbf{q})$ (i.e., red and green solid lines in Fig. 4). We have found that in this fixed $\lambda_{\rm dyn}$ case $\Delta E/E$ is comparatively smaller by a maximum (at $p = 40$ GeV/c) of 4.4% and 3.8% in the MIS and CE methods, respectively. This can be easily understood from Fig. 2 where the energy loss for $\lambda_{\rm dyn}$ computed at $T = 0.235$ GeV (corresponding to $\tau \approx 2.16$ fm/c) has a lower value, and accordingly the time-integrated $E^{-1}dE/d\tau$ receives a smaller contribution at small τ as compared to temperature-dependent $\lambda_{\rm dyn}(T)$. Furthermore, we find from Fig. 4 that the inclusion of $\delta\Lambda_{\rm vis}(\tau,\mathbf{q})$ causes $\Delta E/E$ to increase by a maximum of 14.9% and 7.9% in the MIS and CE methods, respectively, as compared to the $\delta\Lambda_{\rm vis} = 0$ case. Hence, $\delta\Lambda_{\rm vis}(\tau,\mathbf{q})$ affects more the fractional radiative energy loss relative to the temperature-dependent $\lambda_{\rm dyn}(T)$.

It is important to note that, in a nonexpanding medium, the total energy loss can be expressed as $\Delta E \sim \mathcal{S}(E)\int dL/(3\alpha_s T)$, where $\mathcal{S}(E)$ is a function of the energy of the charm quark. Hence the total energy loss increases linearly with the path-length L traversed by the quark which is a QCD analog of the QED Bethe-Heitler limit [11]. On the other hand, the corresponding energy loss for a time-dependent viscous medium may be written as $\Delta E \sim \int d\tau\, \mathcal{C}(E,\tau,\eta)/[3\alpha_s T(\tau)]$, where $\mathcal{C}(E,\tau,\eta)$ is a complicated function encompassing medium effects. Figure 5 illustrates the time dependence of the fractional energy loss in the ideal and dissipative hydrodynamics with $T_0 = 0.400$ GeV. The corresponding energy loss for a nonexpanding medium at an average temperature of $T_0 = 0.228$ GeV (the same as used in Fig. 4) is shown as a function of the effective thickness of the medium. We find that the expanding medium shows a nonlinear behavior in the fractional energy loss which has been also observed in a complementary approach pertaining to coherent gluon radiation from the finite-size nonexpanding QCD medium consisting of static scatterers [58].

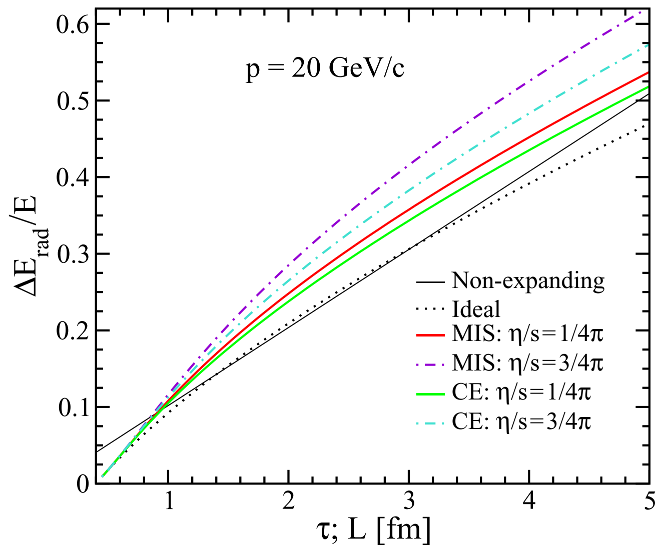

FIG. 5. Time dependence of fractional radiative energy loss for charm quarks of initial momentum $p = 20$ GeV/c with viscous corrections included in the distribution function in models of dissipative hydrodynamics. The initial conditions and the various curves are the same as in Fig. 4.

IV. SUMMARY

In this paper we have presented a theoretical formulation of the radiative energy loss of a heavy quark traversing in a viscous medium that undergoes boost-invariant longitudinal expansion. The calculation was performed in first order in opacity for a dynamically screened QCD plasma at finite temperatures. We have derived the radiative energy loss by including two forms of viscous correction in the nonequilibrium phase-space distribution, namely, Grad's 14-moment approximation and the Chapman-Enskog-like iterative solution. The evolution of the medium was treated within relativistic second-order viscous hydrodynamics based on the MIS framework, that uses Grad's approximation for the distribution function, and the CE method.

Viscous contributions from dynamics only, in the absence of viscous corrections in the single-particle phase-space distribution, resulted in the enhancements of the fractional differential energy-loss energy by about $\sim$5% depending on the shear viscosity to entropy density ratio of $\eta/s = 0.08$–0.24 used. This energy loss was found to be similar in the MIS and CE dissipative hydrodynamic models. At the early stages of evolution, we found that inclusion of Grad's approximation of the viscous correction in the distribution function resulted in an appreciably large increase in fractional energy loss that increased monotonically with momentum p of the charm quark. On the other hand, in the Chapman-Enskog viscous correction, the enhancement was found to be comparatively smaller, and the energy loss was seen to saturate for $p \gtrsim 10$ GeV/c. At later proper times, the energy losses in all the scenarios were found comparable due to low temperatures and the nearly vanishing shear stress tensor. The time-integrated fractional energy loss in Grad's approximation was found higher than in the Chapman-Enskog method. The heavy quark radiative energy-loss results presented in this paper are crucial for the interpretation of the D-meson nuclear modification factor.

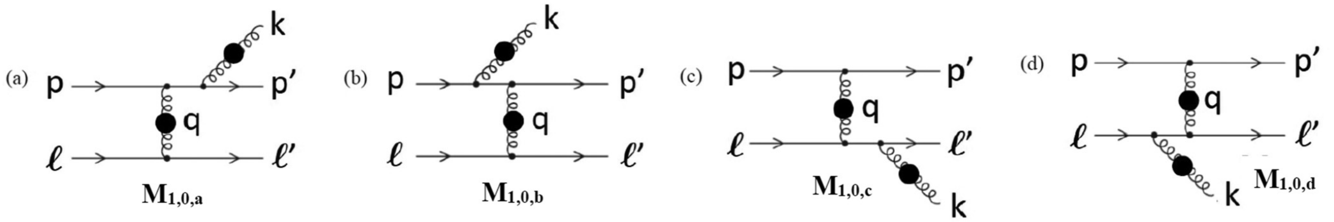

FIG. 6. (a)–(d) Feynman diagrams $M_{1,0}$ contributing to heavy quark radiative energy loss to first order in opacity.

ACKNOWLEDGMENTS

The authors thank A. Jaiswal for useful discussions. S.S. acknowledges support from DST-INSPIRE Faculty award.

APPENDIX A: POLARIZATION TENSOR IN A VISCOUS QCD PLASMA

We calculate the gluon polarization tensor in the presence of a nonequilibrium single-particle distribution function due to Grad's method [44]. The viscous correction of the polarization tensor is calculated in the 1-HTL approach within viscous hydrodynamics. For this one-loop order, the polarization tensor of the gluons of momentum $l=(l_0,\vec{\mathbf{l}})$ has contributions from four diagrams, which for an equilibrated plasma is given by [55,56]

$$\Pi_{\mu\nu}(l) = -2g^2\int \frac{d^3p}{|\vec{\mathbf{p}}|(2\pi)^3}[N_f f_+(p)+N_c f_-(p)] \times\left(-\delta^0_\mu\delta^0_\nu + l_0\frac{\hat{p}_\mu\hat{p}_\nu}{l_0-\hat{\mathbf{p}}\cdot\vec{\mathbf{l}}+i\eta}\right). \tag{A1}$$

To mimic a plasma of quarks and gluons, we have considered a gas of fermions and bosons with distribution functions $f_+(p)$ and $f_-(p)$, respectively. The nonzero components of the polarization tensor are the longitudinal $\Pi_L=-\Pi_{00}$ and transverse $\Pi_T=(\delta_{ij}-l_il_j/\vec{\mathbf{l}}^2)\Pi_{ij}/2$ ones.

In the presence of a viscous correction due to Grad (5) and in-medium modifications [50], the fermionic and bosonic distribution functions become

$$f(p) = f_0(p) + \frac{3\Phi}{4sT^3}\left[\frac{\mathbf{p}^2+p_z^2(\tau_0/\tau)^2}{3} - p_z^2\frac{\tau_0^2}{\tau^2}f_0(p)[1\pm f_0(p)]\right], \tag{A2}$$

where the plus and minus signs refer to fermions and bosons and $p_z=|\vec{\mathbf{p}}|\cos\theta_p$. We have introduced a dimensionless variable $y=p_z/|\vec{\mathbf{p}}|$, which can be also written as

$$y\equiv y(p) = \frac{|\vec{\mathbf{p}}|\cos\theta_p(\tau_0/\tau)}{\sqrt{\vec{\mathbf{p}}^2\cos^2\theta_p(\tau_0/\tau)^2+\vec{\mathbf{p}}^2}}. \tag{A3}$$

Limits on y are decided by $\cos\theta_p$ viz. $y\in[y_{\min},y_{\max}]$. On substituting the distribution function we obtain

$$\Pi_L(l) = \Pi_L^0(l) - \frac{3\Phi}{4sT^3}\frac{2g^2}{(2\pi)^2}\int_0^\infty \mathbf{p}^3 d\mathbf{p}\int_{y_{\min}}^{y_{\max}} dy \times\left(\frac{N_f}{e^{g(\mathbf{p})}+1}+\frac{N_c}{e^{g(\mathbf{p})}-1}\right)\frac{1-3y^2}{3(1-y)^2}\frac{|\vec{\mathbf{l}}|y}{l_0-|\vec{\mathbf{l}}|y},$$

$$\Pi_T(l) = \Pi_T^0(l) - \frac{3\Phi}{4sT^3}\frac{g^2}{(2\pi)^2}\int_0^\infty \mathbf{p}^3 d\mathbf{p}\int_{y_{\min}}^{y_{\max}} dy \times\left(\frac{N_f}{e^{g(\mathbf{p})}+1}+\frac{N_c}{e^{g(\mathbf{p})}-1}\right)\frac{1-3y^2}{3(1-y)^2}\frac{|\vec{\mathbf{l}}|(1-y)}{l_0-|\vec{\mathbf{l}}|y}. \tag{A4}$$

Here $g(\mathbf{p}) =: \mathbf{p}/(T\sqrt{1-y^2})$, and the usual ideal parts for the longitudinal and transverse self-energies [55,56] are as follows:

$$\Pi_T^0(l) = \mu^2\left[\frac{y'^2}{2}+\frac{y'(1-y'^2)}{4}\ln\left(\frac{y'+1}{y'-1}\right)\right],$$
$$\Pi_L^0(l) = \mu^2\left[1-y'^2-\frac{y'(1-y'^2)}{4}\ln\left(\frac{y'+1}{y'-1}\right)\right], \tag{A5}$$

with $y'=l_0/|\vec{\mathbf{l}}|$. In the limit of $\eta/s\to 0$, the results for the nonexpanding plasma are recovered. It may be noted from Eq. (A5) that, in the limit of $l_0\to 0$, the longitudinal (electric) polarization gives time-dependent screening and the transverse (magnetic) polarization is Landau damped.

APPENDIX B: COMPUTATION OF DIAGRAMS $\mathcal{M}_{1,0}$ AND ASSOCIATED RADIATIVE ENERGY LOSS IN MIS THEORY

We present a detailed calculation of the first set of diagrams corresponding to $\mathcal{M}_{1,0}$. In general, we denote all the loop diagrams as $\mathcal{M}_{1,i,j}$, where i refers to the number of the exchanged gluon q's that are attached to the radiated gluon k and $j=a,b,\ldots$ denotes the particular diagram in that class, computed in first order in opacity denoted by 1. The Feynman diagrams for the first set, namely, $M_{1,0,a}$, $M_{1,0,b}$, $M_{1,0,c}$, and $M_{1,0,d}$ are shown in Fig. 6. These scattering diagrams are associated with two-cut HTL diagrams. We first compute the cut diagram $\mathcal{M}^>_{1,0,a}=2\,\mathrm{Im}\,\mathcal{M}_{1,0,a}$ (see Fig. 7),

$$\mathcal{M}^>_{1,0,a} = g^4 t_a t_c t_c t_a\int\frac{d^4p'}{(2\pi)^4}\frac{d^4q}{(2\pi)^4}\frac{d^4k}{(2\pi)^4} \times(2p-q)^\mu D^>_{\mu\nu}(q)(2p-q)^\nu[D(p'+k)]^2 \times(2p'+k)^\rho D^>_{\rho\sigma}(k)(2p'+k)^\sigma D^>(p') \times(2\pi)^4\delta^4(p-p'-k-q). \tag{B1}$$

The above equation consists of two parts: the medium interaction and the phase-space factor. The interaction history is encoded in the exchanged and radiated gluon propagators $D_{\mu\nu}(q)$ and $D_{\rho\sigma}(k)$, respectively; $D(p')$, $D(p'+k)$ are the

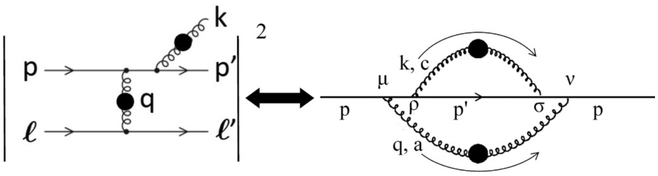

FIG. 7. Left: Scattering amplitude of the $M_{1,0,a}$ diagram where a heavy quark of momentum p suffers collisional interaction with medium partons of momentum l via a screened gluon of momentum q, resulting in the emission of a gluon of momentum k from the outgoing quark. The corresponding momenta of the scattered states are denoted by p' and l'. The blob represents the medium modified gluon propagator. Right: HTL loop diagram of first order in opacity corresponding to $\mathcal{M}_{1,0,a}$. Heavy quark scatterers from medium partons via the cut gluon propagator of momentum q (with $q_0 \leqslant |\vec{\mathbf{q}}|$) resulting in the emission of a cut gluon propagator with momentum k (with $\omega > |\vec{\mathbf{k}}|$). The imaginary part of the diagram corresponds to the squared amplitude of the left diagram and is integrated over phase space.

fermionic propagators. To proceed further we write the vector contraction as

$$(2p'+k)^\rho P_{\rho\sigma}(k)(2p'+k)^\sigma$$
$$\approx 2p'^\rho P_{\rho\sigma}(k) 2p'^\sigma \approx -4\left(\vec{\mathbf{p}}'^2 - \frac{(\vec{\mathbf{p}}'\cdot\vec{\mathbf{k}})^2}{|\vec{\mathbf{k}}|^2}\right), \tag{B2}$$

where we have used $k^\rho P_{\rho\sigma}(k) = 0$. By choosing the coordinate axis $\vec{\mathbf{q}} = |\vec{\mathbf{q}}|(\sin\theta_q\cos\phi_q, \sin\theta_q\sin\phi_q, \cos\theta_q)$, $\vec{\mathbf{k}} = |\vec{\mathbf{k}}|(\sin\theta_k\cos\phi_k, \sin\theta_k\sin\phi_k, \cos\theta_k)$ and $\vec{\mathbf{p}}'$ along the z direction, one can evaluate the terms within the braces of Eq. (B2) as

$$\vec{\mathbf{p}}'^2 - \frac{(\vec{\mathbf{p}}'\cdot\vec{\mathbf{k}})^2}{|\vec{\mathbf{k}}|^2} \approx \frac{p_z'^2\mathbf{k}^2}{\mathbf{k}^2 + p_z'^2x^2} \approx \frac{\mathbf{k}^2}{x^2}, \tag{B3}$$

where $x =: k_z/p'_z$. Similarly, for the vector contraction with the exchanged gluon term one can write

$$p^\mu \mathrm{Im}\, P_{\mu\nu} p^\nu \approx -\frac{E^2\mathbf{q}^2}{\mathbf{q}^2 + q_z^2} \approx -p^\mu\, \mathrm{Im}\, Q_{\mu\nu} p^\nu. \tag{B4}$$

Other approximations which we use are $q_z \sim |\mathbf{q}|$, $|\mathbf{k}| \ll k_z$, $q_z \ll k_z$. The longitudinal component of the emitted and radiated gluons obeys the following approximations: $k_z + q_z \approx k_z$, $p'_z + k_z + q_z \approx p'_z + k_z \approx p'_z$ and $p'_z + q_z \approx p'_z$. For the energy δ function we thus obtain

$$\delta(E - E' - \omega - q_0) \approx \delta(q_z - q_0). \tag{B5}$$

While writing the above equation it has been assumed that $M^2/2p_z'^2 \ll 1$, $(\mathbf{k}^2 + m_g^2)/2k_z \ll 1$, $[(\mathbf{k}+\mathbf{q})^2 + M^2]/2p'_z \ll 1$. Similarly, for the propagator one can write

$$(p'+k)^2 - M^2 = 2\left(p'_z + \frac{(\mathbf{k}+\mathbf{q})^2 + M^2}{2p'_z}\right)$$
$$\times\left(k_z + \frac{\mathbf{k}^2 + m_g^2}{2k_z}\right)$$
$$- 2[k_z p'_z + \mathbf{k}\cdot(-\mathbf{k}-\mathbf{q})],$$
$$\approx \frac{\mathbf{k}^2 + M^2x^2 + m_g^2}{x}. \tag{B6}$$

By using Eqs. (B2)–(B6) along with Eqs. (14) and (15), Eq. (B1) reduces to

$$\mathcal{M}^{>}_{1,0,a} = 16g^4 t_a t_c t_c t_a \int \frac{dp'_0}{2\pi}\frac{d^4q}{(2\pi)^4}\frac{d^4k}{(2\pi)^4}$$
$$\times \frac{\mathbf{k}^2}{\left(\mathbf{k}^2 + M^2x^2 + m_g^2\right)^2}(1 + f_q)\frac{E^2\mathbf{q}^2}{\mathbf{q}^2 + q_z(\tau)^2}$$
$$\times\left\{2\,\mathrm{Im}\left(\frac{1}{q^2 - \Pi_L(q)}\right) - 2\,\mathrm{Im}\left(\frac{1}{q^2 - \Pi_T(q)}\right)\right\}$$
$$\times 2\pi\frac{\delta(p'_0 - E')}{2E'}2\pi\frac{\delta(k_0 - \omega)}{2\omega}$$
$$\times 2\pi\delta(p_0 - p'_0 - k_0 - q_0)\theta\left(1 - \frac{q_0^2}{\vec{\mathbf{q}}^2}\right). \tag{B7}$$

In the high-temperature plasma and small q_0, the equilibrium part $f_0(q)$ of the distribution function $f(q)$ of Eq. (A2), can be approximated as $f_0(q)[1 + f_0(q)] \simeq f_0(q) \simeq 1/(1 + q_0/T - 1) \simeq T/q_0 = T/q_z$. Since $q^2 = q_0^2 - q_z^2 - \mathbf{q}^2$ and using the δ function, we can write $q_0 \sim q_z$, $q^2 \approx -\mathbf{q}^2$. On performing the p_0, k_0, and q_0 integrations and in terms of the dimensionless variable $y \equiv y(q)$ of Eq. (A3), we finally get

$$\mathcal{M}^{>}_{1,0,a} = 8g^4 t_a t_c t_c t_a ET \int \frac{d^3k}{(2\pi)^3 2\omega}\frac{\mathbf{k}^2}{\left(k_\perp^2 + M^2x^2 + m_g^2\right)^2}$$
$$\times \int \frac{\mathbf{q}\, d\mathbf{q}\, dy\, d\phi}{(2\pi)^2}\left(1 + \frac{3\Phi}{4sT^3}\frac{\mathbf{q}^2(1-3y^2)}{3(1-y^2)}\right)$$
$$\times\left\{\frac{2\,\mathrm{Im}\,\Pi_L(y)}{[\mathbf{q}^2 + \mathrm{Re}\,\Pi_L(y)]^2 + [\mathrm{Im}\,\Pi_L(y)]^2}\right.$$
$$\left. - \frac{2\,\mathrm{Im}\,\Pi_T(y)}{[\mathbf{q}^2 + \mathrm{Re}\,\Pi_T(y)]^2 + [\mathrm{Im}\,\Pi_T(y)]^2}\right\}. \tag{B8}$$

It can be shown that the contribution from the other three diagrams $\mathcal{M}^{>}_{1,0,b}$, $\mathcal{M}^{>}_{1,0,c}$, $\mathcal{M}^{>}_{1,0,d}$ has the same result but for the color factor. On summing all four diagrams and using Eqs. (8) and (9), the heavy quark radiative energy loss with Grad's viscous correction for this set,

$$\left.\frac{1}{E}\frac{dE}{d\tau}\right|_{1,0} = \frac{2g^4T[t_a,t_c][t_c,t_a]}{(2\pi)^5 D_R}\int_0^1 dx \int_0^{k_{\max}} \mathbf{k}\, d\mathbf{k} \int_0^{2\pi} d\phi_k$$
$$\times \int_0^{q_{\max}} \mathbf{q}\, d\mathbf{q} \int_0^{2\pi} d\phi_q \int_{y_{\min}}^{y_{\max}} dy$$
$$\times \frac{\mathbf{k}^2}{\left(\mathbf{k}^2 + M^2x^2 + m_g^2\right)^2}$$
$$\times\left(1 + \frac{\Phi}{4sT^3}\frac{\mathbf{q}^2(1-3y^2)}{1-y^2}\right)\mathcal{F}_{LT}(\mathbf{q},y). \tag{B9}$$

With the help of the commutator relation $[t_a,t_c][t_c,t_a] = 3C_R D_R$ and defining the strong-coupling constant $\alpha_s = g^2/(4\pi)$, the coefficient in front of the integral can be written as $3\alpha_s^2 C_R T/\pi^3$. We use the notation $\mathcal{F}_{LT} \equiv \mathcal{F}_L - \mathcal{F}_T$ for the difference in the polarization tensors $\mathcal{F}_Z = 2\,\mathrm{Im}\,\Pi_Z(y)\{[\mathbf{q}^2 + \mathrm{Re}\,\Pi_Z(y)]^2 + [\mathrm{Im}\,\Pi_Z(y)]^2\}^{-1}$ with $Z \equiv (L,T)$. The upper limits of integration are set to $q_{\max} = \sqrt{6ET}$ and $k_{\max} = 2E\sqrt{x(1-x)}$ [58].

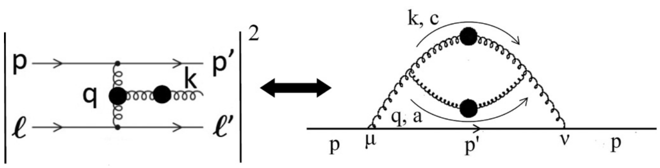

FIG. 8. Feynman diagram $M_{1,2}$ for the heavy quark radiative energy loss to first order in opacity (left) and the corresponding loop diagram $\mathcal{M}_{1,2}$ (right). The notations are the same as in Fig. 7 except that the emission of the gluon of momentum k occurs from the virtual or exchanged gluon of momentum q.

APPENDIX C: COMPUTATION OF DIAGRAM $\mathcal{M}_{1,2}$ AND CORRESPONDING RADIATIVE ENERGY LOSS

We present detailed calculations for a diagram corresponding to $\mathcal{M}_{1,2}$ where both ends of the exchanged gluon q are attached to the radiated gluon (see Fig. 8). The contribution of this diagram is given below, $\mathcal{M}^{>}_{1,2} = 2\,\mathrm{Im}\,\mathcal{M}_{1,2}$,

$$\mathcal{M}^{>}_{1,2} = \frac{g^4}{2E} f^{bac} t_b f^{dac} t_d \int \frac{d^4p'}{(2\pi)^4}\frac{d^4q}{(2\pi)^4}\frac{d^4k}{(2\pi)^4} \times (2\pi)^4\delta^4(p-p'-k-q) D^{>}(p')H, \tag{C1}$$

where we have defined

$$\begin{aligned} H &= (2p-k')^{\mu}(2p-k')^{\nu} D_{\mu\rho}(k')D^{>}_{\lambda\alpha}(k)D^{>}_{\tau\beta}(q)D^{*}_{\sigma\nu}(k') \\ &\quad\times[g^{\rho\tau}(k'+q)^{\lambda} + g^{\lambda\tau}(k-q)^{\rho} - g^{\lambda\rho}(k'+k)^{\tau}] \\ &\quad\times[g^{\sigma\beta}(k'+q)^{\alpha} + g^{\alpha\beta}(k-q)^{\sigma} - g^{\alpha\sigma}(k'+k)^{\beta}]. \end{aligned} \tag{C2}$$

We follow similar algebra for the vector contraction as used in Eqs. (B2)–(B6). The fermionic propagator can then be expressed as

$$\begin{aligned} (k+q)^2 - m_g^2 &= m_g^2 - \mathbf{q}^2 + 2\left(k_z + \frac{\mathbf{k}^2 + m_g^2}{2k_z}\right) \\ &\quad\times\left(q_z - \frac{\mathbf{k}^2 + M^2x^2 + m_g^2}{2k_z}\right) \\ &\quad - 2k_zq_z - 2\mathbf{kq} - m_g^2, \\ &\approx -\left[(\mathbf{k}+\mathbf{q})^2 + M^2x^2 + m_g^2\right]. \end{aligned} \tag{C3}$$

Furthermore, using $if^{bac}t_b = [t_a,t_c]$ and the viscous correction due to Grad [see Eq. (A2)], one can compute the diagram of Eq. (C1). The corresponding radiative energy loss in Grad's 14-moment approximation,

$$\begin{aligned} \frac{1}{E}\frac{dE}{d\tau}\bigg|_{1,2} &= \frac{2g^4T[t_a,t_c][t_c,t_a]}{(2\pi)^5 D_R}\int_0^1 dx\int_0^{k_{\max}} \mathbf{k}\,d\mathbf{k}\int_0^{2\pi} d\phi_k \\ &\quad\times\int_0^{q_{\max}} \mathbf{q}\,d\mathbf{q}\int_0^{2\pi} d\phi_q\int_{y_{\min}}^{y_{\max}} dy \\ &\quad\times\frac{(\mathbf{k}+\mathbf{q})^2}{\left[(\mathbf{k}+\mathbf{q})^2 + M^2x^2 + m_g^2\right]^2} \\ &\quad\times\left(1 + \frac{\Phi}{4sT^3}\frac{\mathbf{q}^2(1-3y^2)}{1-y^2}\right)\mathcal{F}_{LT}(\mathbf{q},y). \end{aligned} \tag{C4}$$

APPENDIX D: COMPUTATION OF DIAGRAMS $\mathcal{M}_{1,1}$ AND CORRESPONDING RADIATIVE ENERGY LOSS

We present calculations of the diagrams $\mathcal{M}_{1,1}$ where one of the ends of the exchanged gluon q is attached to the radiated gluon. This can be evaluated as the product of the previous two diagrams (see Fig. 9). For the first diagram $\mathcal{M}^{>}_{1,1,a}$ one can express

$$\begin{aligned} \mathcal{M}^{>}_{1,1,a} &\approx \frac{g^4}{2E} f^{cba} t_b t_c t_a \int \frac{d^4p'}{(2\pi)^4}\frac{d^4q}{(2\pi)^4}\frac{d^4k}{(2\pi)^4} \\ &\quad\times\frac{1}{(p'+k)^2 - M^2 - i\epsilon}(2\pi)^4\delta^4(p-p'-k-q) \\ &\quad\times D^{>}(p')G, \end{aligned} \tag{D1}$$

where we denote

$$\begin{aligned} G &\approx [(2p-k')^{\mu}(2p'+k)^{\nu}(2p-q)^{\sigma} \\ &\quad\times D_{\mu\rho}(k')D^{>}_{\nu\lambda}(k)D^{>}_{\sigma\tau}(q)] \\ &\quad\times[g^{\rho\tau}(k'+q)^{\lambda} + g^{\lambda\tau}(k-q)^{\rho} - g^{\lambda\rho}(k'+k)^{\tau}], \\ &\equiv G_1 + G_2 - G_3. \end{aligned} \tag{D2}$$

Here,

$$\begin{aligned} G_1 &= [(2p-k')_{\mu}D^{\mu\rho}(k')D^{>}_{\rho\sigma}(q)(2p-q)^{\sigma}] \\ &\quad\times[(k'+q)^{\lambda}D^{>}_{\lambda\nu}(k)(2p'+k)^{\nu}], \end{aligned} \tag{D3}$$

$$\begin{aligned} G_2 &= [(2p-k')^{\mu}D_{\mu\rho}(k')(k-q)^{\rho}] \\ &\quad\times[(2p'+k)^{\nu}D^{>}_{\nu\lambda}(k)D^{>}_{\lambda\sigma}(q)(2p-q)_{\sigma}], \end{aligned} \tag{D4}$$

$$\begin{aligned} G_3 &\approx [(2p-k')_{\mu}D^{\mu\rho}(k')D^{>}_{\rho\nu}(k)(2p'+k)^{\nu}] \\ &\quad\times[(k+k')^{\tau}D^{>}_{\tau\sigma}(q)(2p-q)^{\sigma}]. \end{aligned} \tag{D5}$$

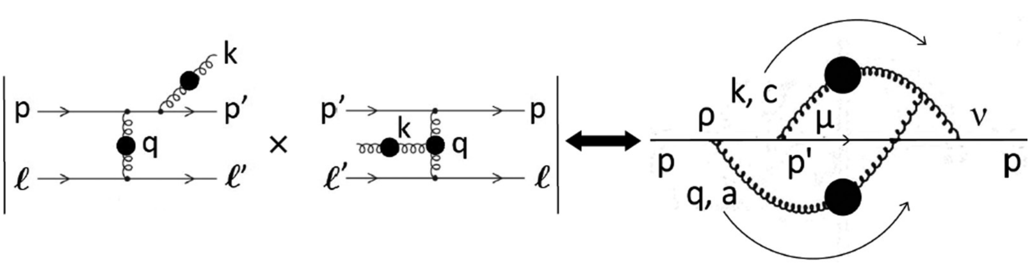

FIG. 9. Feynman diagram $M_{1,1}$ for the heavy quark radiative energy loss to first order in opacity computed as a product of the diagrams in Figs. 7 and 8 (left) and the corresponding loop diagram $\mathcal{M}_{1,1}$ (right).

We consider only G_3 as it gives a dominant contribution in the approximations involving the kinematics noted in Appendix B. With the help of the above equations and viscous correction Eq. (A2), one can compute the energy loss for the diagram $\mathcal{M}^{>}_{1,1,a}$. The energy loss for the other diagrams in this set $\mathcal{M}^{>}_{1,1,b}$, $\mathcal{M}^{>}_{1,1,c}$, $\mathcal{M}^{>}_{1,1,d}$ can be calculated accordingly. On summing all four diagrams we get the total energy loss for this set as

$$\frac{1}{E}\frac{dE}{d\tau}\bigg|_{1,1} = \frac{2g^4T[t_a,t_c][t_c,t_a]}{(2\pi)^5 D_R}\int_0^1 dx\int_0^{k_{\max}}\mathbf{k}\,d\mathbf{k}\int_0^{2\pi}d\phi_k\int_0^{q_{\max}}\mathbf{q}\,d\mathbf{q}\int_0^{2\pi}d\phi_q\int_{y_{\min}}^{y_{\max}}dy \times\frac{-2\mathbf{k}\cdot(\mathbf{k}+\mathbf{q})}{\big[(\mathbf{k}+\mathbf{q})^2+M^2x^2+m_g^2\big]\big[\mathbf{k}^2+M^2x^2+m_g^2\big]}\left(1+\frac{\Phi}{4sT^3}\frac{\mathbf{q}^2(1-3y^2)}{1-y^2}\right)\mathcal{F}_{LT}(\mathbf{q},y). \tag{D6}$$

[1] J. Adams *et al.* (STAR Collaboration), Nucl. Phys. A **757**, 102 (2005).
[2] K. Adcox *et al.* (PHENIX Collaboration), Nucl. Phys. A **757**, 184 (2005).
[3] K. Aamodt *et al.* (ALICE Collaboration), Phys. Rev. Lett. **107**, 032301 (2011).
[4] G. Aad *et al.* (ATLAS Collaboration), Phys. Rev. C **86**, 014907 (2012).
[5] S. Chatrchyan *et al.* (CMS Collaboration), Phys. Rev. C **89**, 044906 (2014).
[6] P. Romatschke and U. Romatschke, Phys. Rev. Lett. **99**, 172301 (2007).
[7] B. Schenke, S. Jeon, and C. Gale, Phys. Rev. C **85**, 024901 (2012).
[8] Z. Qiu, C. Shen, and U. Heinz, Phys. Lett. B **707**, 151 (2012).
[9] R. S. Bhalerao, A. Jaiswal, and S. Pal, Phys. Rev. C **92**, 014903 (2015).
[10] M. Gyulassy, M. Plümer, M. Thoma, and X. N. Wang, Nucl. Phys. A **538**, 37C (1992); X. N. Wang and M. Gyulassy, Phys. Rev. Lett. **68**, 1480 (1992).
[11] R. Baier, Y. L. Dokshitzer, A. H. Mueller, S. Peigne, and D. Schiff, Nucl. Phys. B **483**, 291 (1997); **484**, 265 (1997).
[12] Z. Lin, R. Vogt and X.-N. Wang, Phys. Rev. C **57**, 899 (1998); Z. Lin and R. Vogt, Nucl. Phys. B **544**, 339 (1999).
[13] R. Baier, D. Schiff, and B. G. Zakharov, Ann. Rev. Nucl. Part. Sci. **50**, 37 (2000).
[14] M. Gyulassy, P. Levai, and I. Vitev, Nucl. Phys. B **571**, 197 (2000); **594**, 371 (2000).
[15] M. Djordjevic, M. Gyulassy, R. Vogt, and S. Wicks, Phys. Lett. B **632**, 81 (2006).
[16] J. D. Bjorken, Fermilab Report No. FERMILAB-PUB-82-059-THY, 1982 (unpublished).
[17] X. N. Wang, M. Gyulassy, and M. Plumer, Phys. Rev. D **51**, 3436 (1995).
[18] M. G. Mustafa, Phys. Rev. C **72**, 014905 (2005); M. G. Mustafa and M. H. Thoma, Acta Phys. Hung. A **22**, 93 (2005).
[19] B. Blagojevic and M. Djordjevic, J. Phys. G: Nucl. Part Phys. **42**, 075105 (2015).
[20] Y. L. Dokshitzer and D. E. Kharzeev, Phys. Lett. B **519**, 199 (2001).
[21] L. Adamczyk *et al.* (STAR Collaboration), Phys. Rev. Lett. **113**, 142301 (2014); G. Xie (STAR Collaboration), Nucl. Phys. A **956**, 473 (2016).
[22] J. Adam *et al.* (ALICE Collaboration), J. High Energy Phys. 03 (2016) 081.
[23] J. Wang (CMS Collaboration), Nucl. Part. Phys. Proc. **289-290**, 249 (2017).
[24] M. Djordjevic, Phys. Rev. Lett. **112**, 042302 (2014).
[25] M. Djordjevic and U. Heinz, Phys. Rev. C **77**, 024905 (2008).
[26] M. Djordjevic and U. W. Heinz, Phys. Rev. Lett. **101**, 022302 (2008).
[27] M. Djordjevic, Phys. Rev. C **80**, 064909 (2009).
[28] M. Djordjevic and M. Gyulassy, Phys. Rev. C. **68**, 034914 (2003).
[29] A. B. Migdal, Phys. Rev. **103**, 1811 (1956); L. D. Landau and I. Pomeranchuk, Dokl. Akad. Nauk Ser. Fiz. **92**, 535 (1953); **92**, 735 (1953).
[30] R. Baier, Y. L. Dokshitzer, A. H. Mueller, and D. Schiff, Nucl. Phys. B **531**, 403 (1998); Phys. Rev. C **58**, 1706 (1998).
[31] M. Guylassy, I. Vitev, X.-N. Wang, and B.-W. Zhang, in *Quark-Gluon Plasma 3*, edited by R. C. Hwa and X. N. Wang (World Scientific, Singapore, 2003), p. 123.
[32] S. Sarkar and A. K. Dutt-Mazumder, Phys. Rev. D **88**, 054006 (2013).
[33] Z. Qiu and U. Heinz, Phys. Lett. B **717**, 261 (2012).
[34] C. Chattopadhyay, R. S. Bhalerao, J. Y. Ollitrault, and S. Pal, Phys. Rev. C **97**, 034915 (2018).
[35] K. Dusling and S. Lin, Nucl. Phys. A **809**, 246 (2008).
[36] G. Vujanovic, C. Young, B. Schenke, R. Rapp, S. Jeon, and C. Gale, Phys. Rev. C **89**, 034904 (2014).
[37] R. Baier, A. H. Mueller, and D. Schiff, Phys. Lett. B **649**, 147 (2007).
[38] I. Müller, Z. Phys. **198**, 329 (1967).
[39] W. Israel and J. M. Stewart, Ann. Phys. (NY) **118**, 341 (1979).
[40] A. Muronga, Phys. Rev. C **69**, 034903 (2004).
[41] A. Jaiswal, Phys. Rev. C **87**, 051901 (2013).
[42] R. S. Bhalerao, A. Jaiswal, S. Pal, and V. Sreekanth, Phys. Rev. C **89**, 054903 (2014).
[43] C. Chattopadhyay, A. Jaiswal, S. Pal, and R. Ryblewski, Phys. Rev. C **91**, 024917 (2015).
[44] H. Grad, Commun. Pure Appl. Math. **2**, 331 (1949).
[45] H. Song and U. W. Heinz, Phys. Rev. C **77**, 064901 (2008).
[46] M. A. York and G. D. Moore, Phys. Rev. D **79**, 054011 (2009).
[47] E. Molnar, H. Niemi, and D. H. Rischke, Phys. Rev. D **94**, 125003 (2016).
[48] W. Florkowski, R. Ryblewski, M. Strickland, and L. Tinti, Phys. Rev. C **94**, 064903 (2016).
[49] C. Chattopadhyay, U. Heinz, S. Pal, and G. Vujanovic, Phys. Rev. C **97**, 064909 (2018).
[50] G. D. Moore and D. Teaney, Phys. Rev. C **71**, 064904 (2005).

[51] P. Romatschke and M. Strickland, Phys. Rev. D **71**, 125008 (2005).
[52] E. Braaten and M. H. Thoma, Phys. Rev. D **44**, 2625(R) (1991).
[53] M. Le Bellac, *Thermal Field Theory* (Cambridge University Press, Cambridge, 1996).
[54] J. I. Kapusta, *Finite-Temperature Field Theory* (Cambridge University Press, Cambridge, 1989).
[55] O. K. Kalashnikov and V. V. Klimov, Sov. J. Nucl. Phys. **31**, 699 (1980).
[56] J. P. Blaizot and E. Iancu, Phys. Rep. **359**, 355 (2002).
[57] M. Luzum and P. Romatschke, Phys. Rev. C **78**, 034915 (2008); **79**, 039903(E) (2009).
[58] M. Djordjevic and M. Gyulassy, Nucl. Phys. A **733**, 265 (2004).